Electronic Supplementary Information

Cobalt single atom catalysts for efficient electrosynthesis of hydrogen peroxide

Hui Xu,[†ab] Shengbo Zhang,[†a] Jing Geng,[ab] Guozhong Wang,[a] Haimin Zhang*[a]

[a.] *Key Laboratory of Materials Physics, Centre for Environmental and Energy Nanomaterials, Anhui Key Laboratory of Nanomaterials and Nanotechnology, CAS Center for Excellence in Nanoscience, Institute of Solid State Physics, HFIPS, Chinese Academy of Sciences, Hefei 230031, China. E-mail:* zhanghm@issp.ac.cn

[b.] *University of Science and Technology of China, Hefei 230026, China.*

[†]*These authors contributed equally to this work.*

Contents

1. Experimental section

1.1 Materials and reagents

Cobalt chloride hexahydrate (CoCl$_2$·6H$_2$O), ethylene diamine tetraaceticacid (EDTA) sodium sulphate (Na$_2$SO$_4$) and polyvinylpyrrolidone (PVP) were purchased from Aladdin Chemical Reagent Co., Ltd. Perchloric acid (HClO$_4$), potassium hydroxide (KOH), and isopropanol were purchased from Sinopharm Chemical Reagent Co., Ltd. Commercial carbon cloth was obtained from Shanghai Hesen electric Co., Ltd. All chemical reagents used in the synthesis were analytical grade and without further purification.

1.2 Synthesis of Co-SAs/NC

In a typical synthesis, the cobalt chloride hexahydrate (CoCl$_2$·6H$_2$O, 0.25 g), ethylene diamine tetraaceticacid (EDTA, 1.0 g) and polyvinylpyrrolidone (PVP, 5.0 g) were dissolved in 63.7 mL of isopropanol. The above mixture was then heated to 80 ℃ in an oil bath for 9 h under vigorous stirring to ensure completion of the reaction and to 90 ℃ for another 4 h to evaporate the solvent. Then the obtained product was transferred into the tube furnace and heated to 700 ℃ with a ramping rate of 5 ℃ min^{-1} under N$_2$ atmosphere and maintained for 2 h, followed by natural cooling down to room temperature. The collected solid product was ground with a mortar, followed by a refluxing acid-etching process using 3.0 M HNO$_3$ at 120 ℃ for10 h to remove Co-related nanoparticles and introduce oxygen functional groups. The resultant product was subsequently centrifuged and washed with deionized water and ethanol for several times, then dried overnight for further use.

1.3 Synthesis of NC

The synthesis of nitrogen-doped graphitic carbon (NC) was similar to the synthesis of Co-SAs/NC except for not using the metal precursor and complexing agent. Typically, the polyvinylpyrrolidone (PVP, 5.0 g) was dissolved in 63.7 mL of isopropanol and then heated to 90 ℃ in an oil bath for 10 h to evaporate the solvent. Then the obtained product was transferred into the tube furnace and heated to 700 ℃ with a ramping rate of 5 ℃ min^{-1} under N_2 atmosphere and maintained for 2 h, followed by natural cooling down to room temperature. The collected solid product was ground with a mortar, followed by a refluxing acid-etching process using 3.0 M HNO_3 at 120 ℃ for 10 h to introduce oxygen functional groups. The resultant product was subsequently centrifuged and washed with deionized water and ethanol for several times, then dried overnight for further use.

1.4 Characterization

The crystalline structures of samples were identified by the X-ray diffraction analysis (XRD, Philips X'pert PRO) using Nifiltered monochromatic CuKa radiation ($\lambda K\alpha 1 = 1.5418$ Å) at 40 kV and 40 mA. Raman spectrum of the sample was measured on a Renishaw Micro-Raman Spectroscopy (Renishaw inVia Reflex) using 532 nm laser excitation. Fourier-transform infrared spectroscopy (FT-IR) spectrum of the sample was measured using NEXUS (Thermo Nicolet Corporation). Scanning electron microscope (SEM) images of the sample were obtained using SU8020 (Hitachi, Japan) with an accelerating voltage of 10.0 kV. Transmission electron microscope (TEM) images of the sample were obtained using JEMARM 200F

operating at an accelerating voltage of 200 kV. Nitrogen adsorption-desorption isotherm was measured using an automated gas sorption analyzer (Autosorb-iQ-Cx). The Co single atom content on N-doped graphitic carbon was determined by the inductively coupled plasma atomic emission spectrometer (ICP-AES, ICP-6300, Thermo Fisher Scientific). X-ray photoelectron spectroscopy (XPS) analysis of the sample was performed on an ESCALAB 250 X-ray photoelectron spectrometer (Thermo, America) equipped with Al Kα1, 2 monochromatized radiations at 1486.6 eV X-ray source. Aberration-corrected HAADF-STEM measurements were conducted on a JEM-ARM200F instrument at 200 kV.

1.5 Electrochemical measurements

The electrochemical measurements were performed on a CHI 760E electrochemical workstation (CH Instrumental Corporation, Shanghai, China) with a three-electrode cell and a rotating ring-disk electrode setup (RRDE-3A, ALS Co., Ltd). A RRDE electrode with a glassy carbon electrode (O.D. 4.0 mm) and a platinum ring electrode (I.D. 5.0 mm, O.D. 7.0 mm) was used as the working electrode. Before measurement, the electrode was polished with 0.3 and 0.05 μm alumina suspensions on a polishing cloth and rinsed with deionized water. A Ag/AgCl electrode and Pt wire were used as the reference and counter electrode, respectively. Three electrolytes with 0.1 M KOH, 0.1M Na_2SO_4 and 0.1 M $HClO_4$ were used in this work. The catalyst ink was prepared by dispersing 5.0 mg as-synthesised Co-SAs/NC into 400 μL of ethanol and 20 μL of Nafion solution (5.0 wt.%), followed by ultrasonication for 1 h to get homogeneous ink. Then 10 μL of catalyst ink was drop-casted onto the disk electrode and naturally

dried. The catalyst loading was 0.95 mg cm^{-2}. All potentials of the electrochemical measurements were converted into reversible hydrogen electrode (RHE) by using the following equation:

$$E_{RHE}=E_{Ag/AgCl}+0.059 \times pH+0.197$$

The H$_2$O$_2$ selectivity was obtained from polarization curves in O$_2$-saturated condition at a scan rate of 10 mV s^{-1} at 1600 rpm and the potential of the Pt ring electrode was held at 1.2 V (*vs.* RHE) to oxidize the H$_2$O$_2$ generated on disk electrode. The H$_2$O$_2$ selectivity and the electron transfer number (n) on the RRDE were calculated using the following equations:

$$Selectivity\ (\%) = \frac{200 \times \dfrac{I_r}{N_c}}{I_d + \dfrac{I_r}{N_c}}$$

$$n = \frac{4I_d}{I_d + \dfrac{I_r}{N_c}}$$

where I_r and I_d are the ring current and the disk current, respectively, and N_c is the collection efficiency of the ring electrode (0.39 after calibration by [Fe(CN)$_6$]$^{3-/4-}$ redox system). We also conducted the polarization curves at different rotation speeds and calculated the electron transfer number (*n*) based on the following Koutecky-Levich (K-L) equations:

$$\frac{1}{j} = \frac{1}{j_k} + \frac{1}{j_d} = \frac{1}{j_k} + \frac{1}{B\sqrt{\omega}}$$

$$B = 0.62nFD^{\frac{2}{3}}v^{-\frac{1}{6}}C$$

where j_k and j_d are the kinetic and diffusion-limited current density, respectively, ω is the angular velocity of the electrode (rad s^{-1}), F is the faraday constant (96485 C

mol^{-1}), D is the diffusion coefficient of O$_2$ in the electrolyte (1.9×10^{-5} cm^2 s^{-1}), ν is the kinematic viscosity of the electrolyte (0.01 cm^2 s^{-1}) and C is the concentration of O$_2$ (1.2×10^{-6} mol cm^{-3}). Accordingly, the electron transfer number can be calculated.

1.6 Durability tests and determination of H$_2$O$_2$ concentration

Electrocatalytic H$_2$O$_2$ production was conducted in a two-compartment H-cell with Nafion 117 membrane as separator. Each compartment was filled with 40 mL of electrolyte (*e.g.*, 0.1 M KOH). We used the carbon cloth (1.0×1.0 cm^2) as the working electrode and the catalyst loading amount was 1.0 mg cm^{-2}, Hg/HgO and Pt mesh as the reference electrode and counter electrode, respectively. Before the measurement, the electrolyte in the cathode compartment was purged with O$_2$ for at least 30 min to reach saturated and stirred vigorously to facilitate the mass transport of O$_2$. In order to screen the optimal potential that can produce more H$_2$O$_2$ with a larger faradaic efficiency (FE), we carried out the tests at different potentials for 2 h of reaction. Then, the long-term durability test was conducted under a constant potential (0.5 V *vs.* RHE) for 10 h and the electrolyte was subsequently neutralized with 0.5 M H$_2$SO$_4$ of equal volume. The H$_2$O$_2$ concentration in the electrolyte was quantified by ceric sulfate titration method based on the following reaction:

$$2Ce^{4+} + H_2O_2 \rightarrow 2Ce^{3+} + 2H^+ + O_2$$
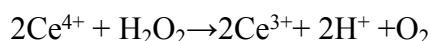
where yellow-colored Ce^{4+} was reduced by H$_2$O$_2$ to colorless Ce^{3+} and can be measured by ultraviolet-visible spectroscopy. A series of standard Ce(SO$_4$)$_2$ solution was prepared by dissolving Ce(SO$_4$)$_2$ in 0.5 M H$_2$SO$_4$, then we obtained the calibration curves between the absorbance and concentration of Ce^{4+} performed on

spectrophotometer at 317 nm. Thus, the concentration of H_2O_2 can be calculated based on the absorbance before and after reaction using the following equation:

$$C_{H_2O_2} = \frac{V_{Ce^{4+}} \times C_{Ce^{4+}_{before}} - \left(V_{Ce^{4+}} + V_{electrolyte}\right) \times C_{Ce^{4+}_{after}}}{2 \times V_{electrolyte}} \times 2 \quad \text{(before neutralization)}$$

where V_{Ce}^{4+} is the volume of added $Ce(SO_4)_2$, $C_{Ce4+ \ before}$ and $C_{Ce4+ \ after}$ are the concentration of Ce^{4+} before and after reaction, respectively, $V_{electrolyte}$ is the volume of added electrolyte which is after neutralization.

The faradaic efficiency was calculated by the following equation:

$$FE \ (\%) = \frac{2 \times C \times V \times F}{Q} \times 100\%$$

where F is the faraday constant (96485 C mol^{-1}), C is the concentration of H_2O_2, V is the volume of electrolyte and Q is the total charge during the ORR.
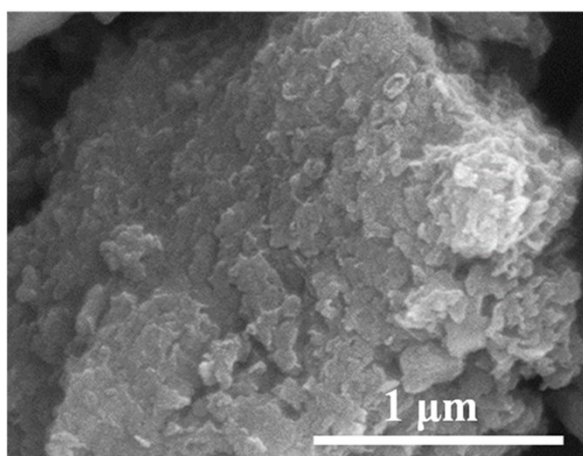
Supplementary Figures and Tables

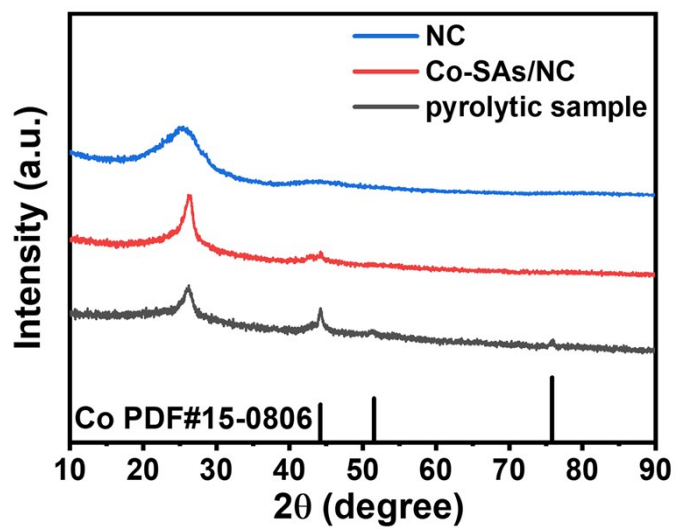**Fig. S1** SEM image of the as-synthesised Co-SAs/NC.

Fig. S2 XRD patterns of N-dope graphitic carbon (NC), Co-SAs/NC and pyrolytic sample without acid etching.
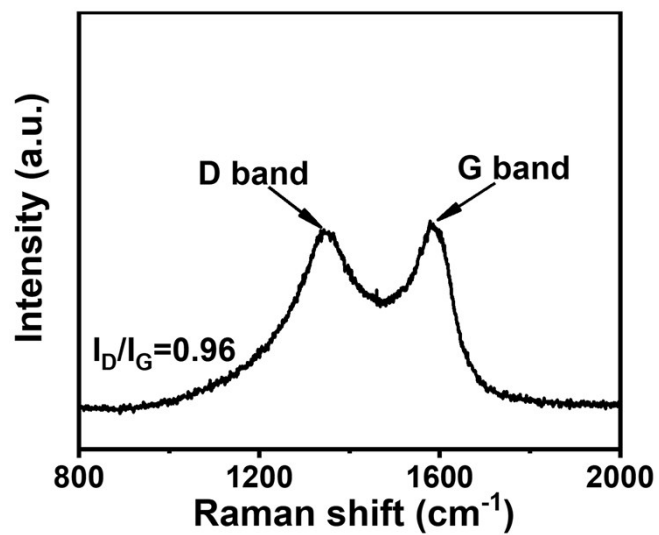
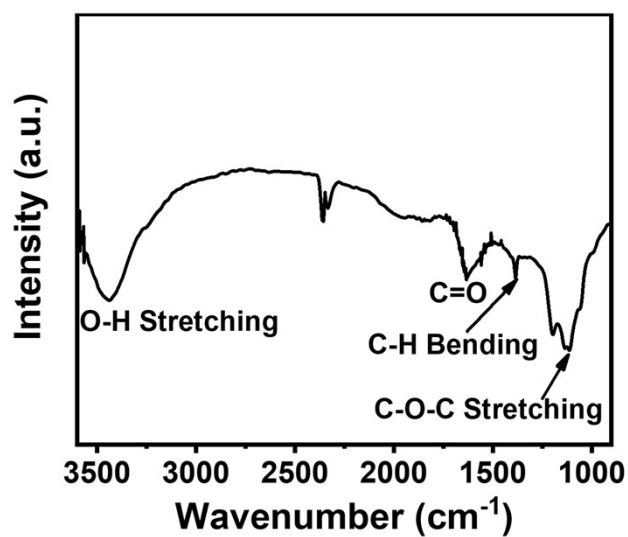**Fig. S3** Raman spectrum of Co-SAs/NC using 532 nm laser excitation.

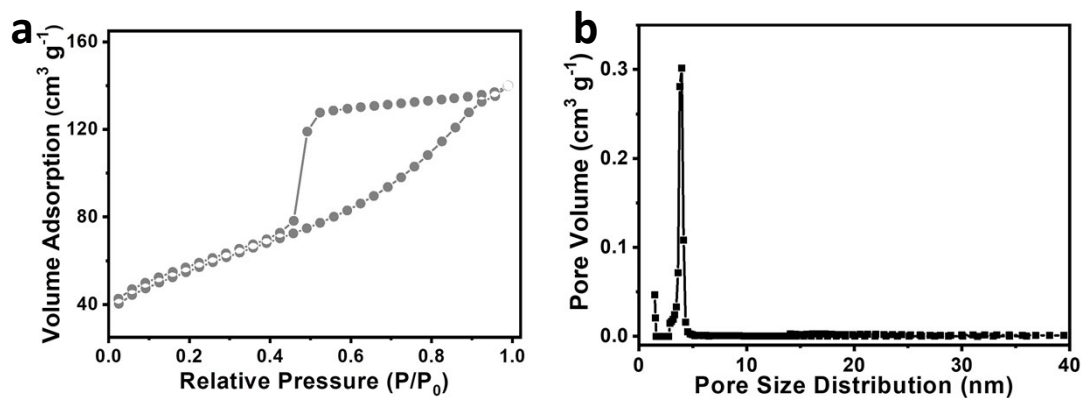**Fig. S4** FT-IR spectrum of Co-SAs/NC sing the KBr pellet technique.

Fig. S5 (a) Nitrogen adsorption-desorption isotherm and (b) Corresponding pore size distribution curve of Co-SAs/NC.
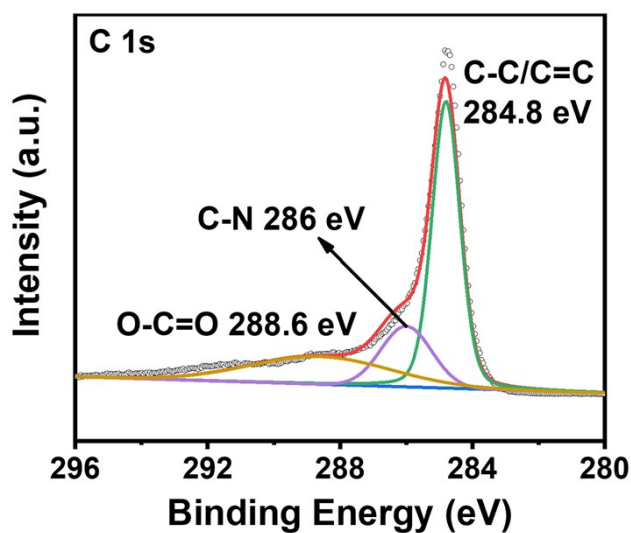

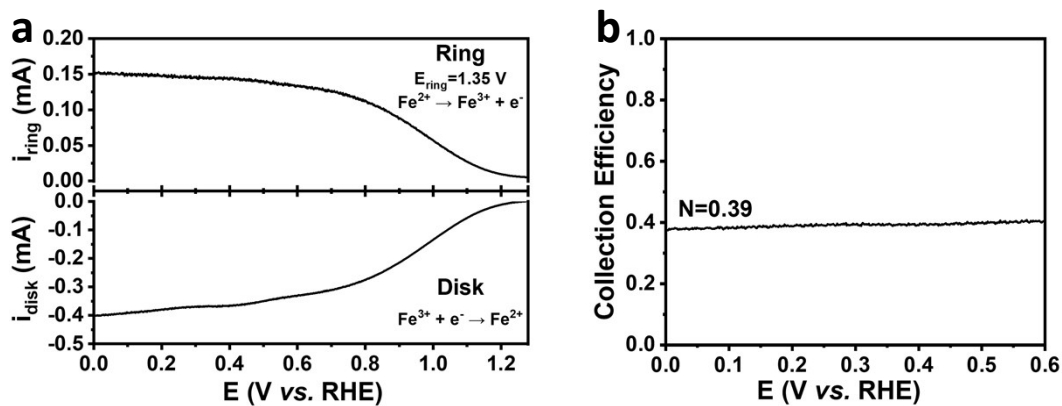**Fig. S6** High-resolution C 1s XPS spectrum of Co-SAs/NC.

Fig. S7 (a) Linear sweep voltammetry curves of the bare rotating ring-disk electrode in N_2-saturated 0.1 M KOH containing 5.0 mM $K_3[Fe(CN)_6]$ at 1600 rpm to calibrate the collection efficiency. (b) Calculated collection efficiency (N) based on LSV result *via* dividing the ring current by the disk current.
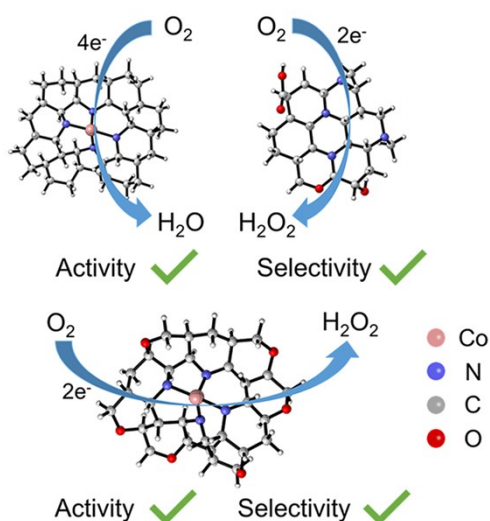

Fig. S8 Schematic illustration of the synergetic effect of Co-N_x active sites and nearby oxygen functional groups for H_2O_2 electrosynthesis.

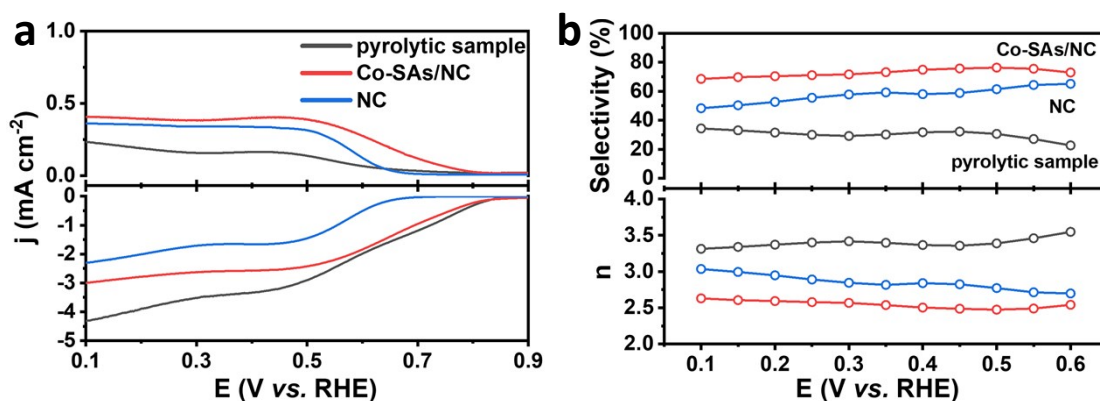**Fig. S9** (a) Linear sweep voltammetry curves of Co-SAs/NC, pyrolytic sample and N-doped graphitic carbon (NC) in 0.1 M KOH. (b) Calculated H_2O_2 selectivity and electron transfer number (n) ofCo-SAs/NC, pyrolytic sample and N-doped graphitic carbon (NC).
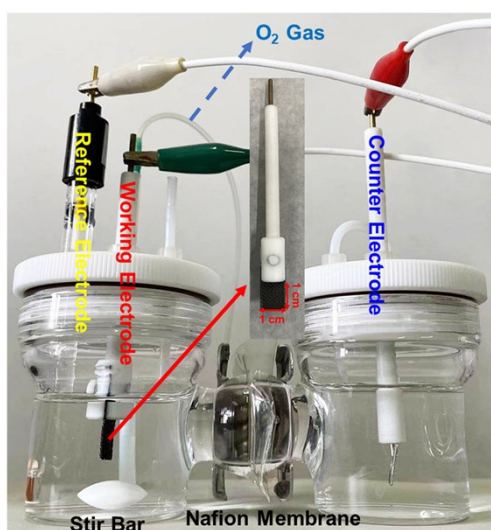

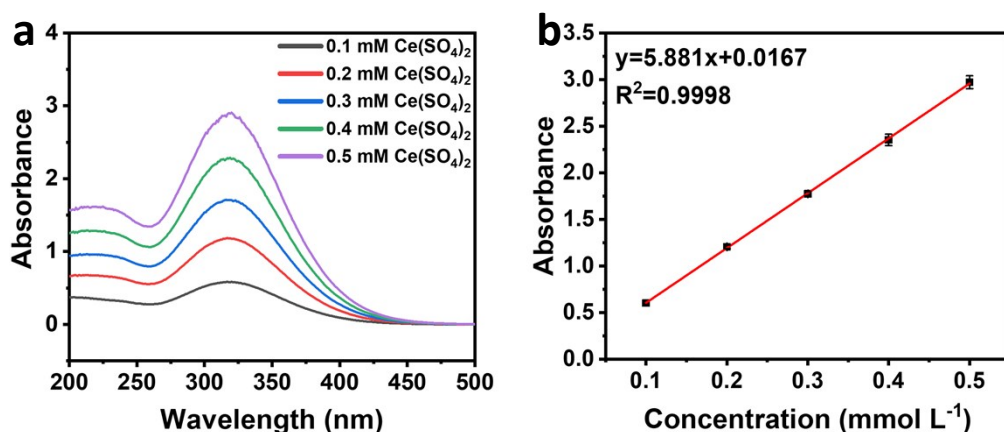**Fig. S10** Digital photograph of the three-electrode two-compartment H-cell for the bulk electrocatalytic production of H_2O_2.

Fig. S11 (a) Absorption spectra of a series of $Ce(SO_4)_2$ solutions with known concentration conducted on ultraviolet-visible spectrophotometer (UV-2700) at the range of 200-500 nm. (b) Linear calibration curve based on the peak absorbance at 317 nm (the error bar represents three replicated measurements).

Fig. S12 (a) Absorption spectra of $Ce(SO_4)_2$ solution before and after injecting electrolytes electrolyzed at different potentials with 2 h, which was conducted on ultraviolet-visible spectrophotometer (UV-2700) at the range of 200-500 nm. To calculate the yield of H_2O_2, we added 200 μL of electrolyte at different potentials after neutralization into 3.0 mL of 0.5 mM $Ce(SO_4)_2$ solution. (b) Absorption spectra of $Ce(SO_4)_2$ solution before and after injecting electrolyte electrolyzed at 0.5 V (*vs*. RHE) with 10 h, which was conducted on ultraviolet-visible spectrophotometer (UV-2700) at the range of 200-500 nm. To calculate the yield of H_2O_2, we added 50 μL of electrolyte after neutralization into 3.0 mL of 0.5 mM $Ce(SO_4)_2$ solution.
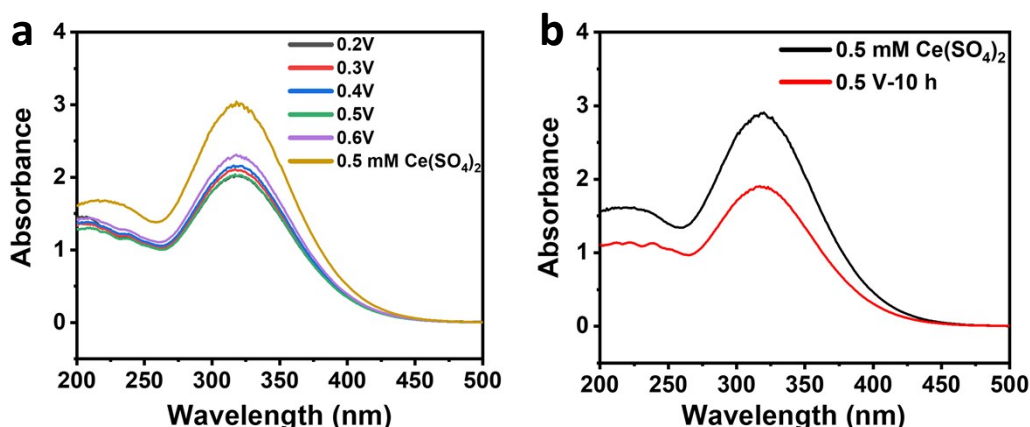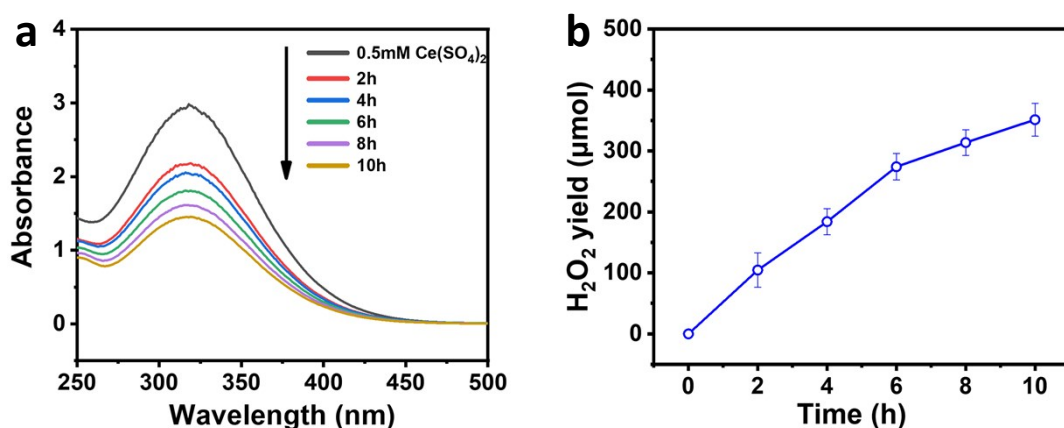
Fig. S13 (a) Absorption spectra of $Ce(SO_4)_2$ solution before and after injecting electrolytes electrolyzed at different time at 0.5 V (*vs.* RHE), which was conducted on ultraviolet-visible spectrophotometer (UV-2700) at the range of 250-500 nm. (b) Relationship between electrolysis time and H_2O_2 yield. To calculate the yield of H_2O_2, we sampled out 100 μL of electrolyte injecting into 6.0 mL of 0.5 mM $Ce(SO_4)_2$ solution every two hours.
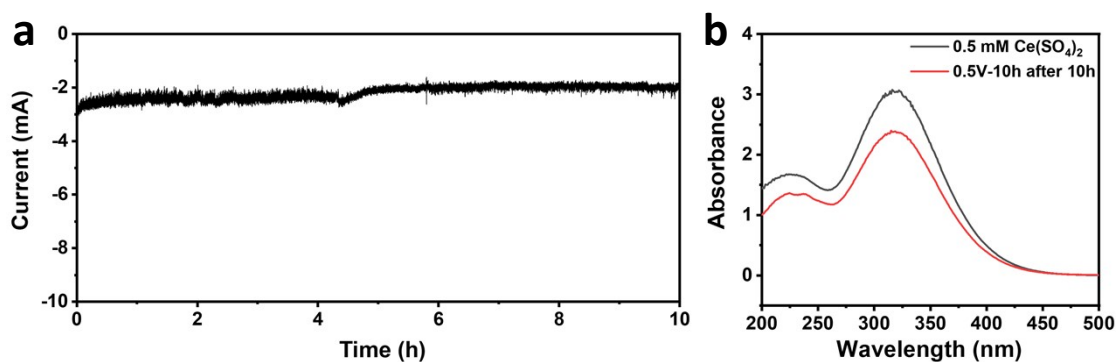
Fig. S14 (a) I-t curve of Co-SAs/NC after 10 h of electrolysis at 0.5 V (*vs.* RHE) for 10 h of reaction. (b) Absorption spectra of $Ce(SO_4)_2$ solution before and after injecting electrolyte electrolyzed at 0.5 V (*vs.* RHE) with 10 h, which was conducted on ultraviolet-visible spectrophotometer (UV-2700) at the range of 200-500 nm. To calculate the yield of H_2O_2, we added 50 μL of electrolyte after neutralization into 3.0 mL of 0.5 mM $Ce(SO_4)_2$ solution.

Table S1. Activity and selectivity comparison of our work and other reported $2e^-$ ORR electrocatalysts.

Catalyst	Electrolyte	Onset potential (V $vs.$ RHE)	Selectivity (%)	References
Co_1-NG(O)	0.1 M KOH	~0.83	82	1
Co-POC-O	0.1 M KOH	0.84	~84	2
Pt/TiN	0.1 M $HClO_4$	~0.60	65	3
Pt/TiC	0.1 M $HClO_4$	~0.60	68	4
h-Pt_1-CuS_x	0.1 M $HClO_4$	~0.70	96	5
Pt/HSC	0.1 M $HClO_4$	0.71	96	6
Mo_1/OSG-H	0.1 M KOH	0.78	95	7
Ni-N_2O_2/C	0.1 M KOH	~0.70	96	8
Ni-SA/G-0	0.1 M KOH	0.74	94	9
G/CDs	0.1 M KOH	0.85	82	10
HPCS-S	0.1 M KOH	0.77	70	11
G-COF-950	0.1 M KOH	~0.74	75	12
CoS_2	0.05 M H_2SO_4	0.69	~70	13
OCB-120	0.1 M KOH	0.80	63.5	14
Co-SAs/NC	**0.1 M KOH**	**0.84**	**76**	**This work**

Table S2. Comparison of H_2O_2 yield using H-cell of our work and other reported $2e^-$ ORR electrocatalysts.

Catalyst	Electrolyte	Potential (V *vs.* RHE)	Electrolysis time (h)	Production rate (mmol g_{cat}^{-1} h^{-1})	FE (%)	References
Pt/HSC	1 M HClO$_4$	0	6	16.67	-	6
Ni-N$_2$O$_2$/C	0.1 M KOH	0.4	8	45.1	85	8
CoS$_2$/CFP	0.05 M H$_2$SO$_4$	0.5	1	38.56	41.2	13
rGO/PEI	0.1 M KOH	0.74	0.5	106.4	90.7	15
o-CoSe$_2$/CFP	0.05 M H$_2$SO$_4$	0.5	6	15.18	53.5	16
c-CoSe$_2$/CFP	0.05 M H$_2$SO$_4$	0.5	5	8.08	7.1	16
Co-SAs/NC	**0.1 M KOH**	**0.5**	**10**	**38.1±1.5 or 17318±682 mmol g_{Co}^{-1} h^{-1}**	**72.1±4.2%**	**This work**

References

1 E. Jung, H. Shin, B. H. Lee, V. Efremov, S. Lee, H. S. Lee, J. Kim, W. Hooch Antink, S. Park, K. S. Lee, S. P. Cho, J. S. Yoo, Y. E. Sung and T. Hyeon, Atomic-level tuning of Co-N-C catalyst for high-performance electrochemical H_2O_2 production, *Nat. Mater.*, 2020, **19**, 436-442.

2 B. Q. Li, C. X. Zhao, J. N. Liu and Q. Zhang, Electrosynthesis of hydrogen peroxide synergistically catalyzed by atomic Co-N_x-C sites and oxygen functional groups in noble-metal-free electrocatalysts, *Adv. Mater.*, 2019, **31**, 1808173.

3 S. Yang, J. Kim, Y. J. Tak, A. Soon and H. Lee, Single-atom catalyst of platinum supported on titanium nitride for selective electrochemical reactions, *Angew. Chem., Int. Ed.*, 2016, **55**, 2058-2062.

4 S. Yang, Y. J. Tak, J. Kim, A. Soon and H. Lee, Support effects in single-atom platinum catalysts for electrochemical oxygen reduction, *ACS Catal.*, 2017, **7**, 1301-1307.

5 R. Shen, W. Chen, Q. Peng, S. Lu, L. Zheng, X. Cao, Y. Wang, W. Zhu, J. Zhang, Z. Zhuang, C. Chen, D. Wang and Y. Li, High-concentration single atomic Pt sites on hollow CuS_x for selective O_2 reduction to H_2O_2 in acid solution, *Chem*, 2019, **5**, 2099-2110.

6 C. H. Choi, M. Kim, H. C. Kwon, S. J. Cho, S. Yun, H. T. Kim, K. J. Mayrhofer, H. Kim and M. Choi, Tuning selectivity of electrochemical reactions by atomically dispersed platinum catalyst, *Nat. Commun.*, 2016, **7**, 10922.

7 C. Tang, Y. Jiao, B. Shi, J. N. Liu, Z. Xie, X. Chen, Q. Zhang and S. Z. Qiao, Coordination tunes selectivity: two-electron oxygen reduction on high-loading molybdenum single-atom catalysts, *Angew. Chem., Int. Ed.*, 2020, **59**, 9171-9176.

8 Y. Wang, R. Shi, L. Shang, G. I. N. Waterhouse, J. Zhao, Q. Zhang, L. Gu and T. Zhang, High-efficiency oxygen reduction to hydrogen peroxide catalyzed by nickel single-atom catalysts with tetradentate N_2O_2coordination in a three-phase flow cell, *Angew. Chem., Int. Ed.*, 2020, **59**, 13057-13062.

9 X. Song, N. Li, H. Zhang, L. Wang, Y. Yan, H. Wang, L. Wang and Z. Bian, Graphene-supported single nickel atom catalyst for highly selective and efficient hydrogen peroxide production, *ACS Appl. Mater. Interfaces*, 2020, **12**, 17519-17527.

10 Y. Dong, J. Su, S. Zhou, M. Wang, S. Huang, C. H. Lu, H. Yang and F. Fu, Carbon-based dots for the electrochemical production of hydrogen peroxide, *Chem. Commun.*, 2020, **56**, 7609-7612.

11 G. Chen, J. Liu, Q. Li, P. Guan, X. Yu, L. Xing, J. Zhang and R. Che, A direct H_2O_2 production based on hollow porous carbon sphere-sulfur nanocrystal composites by confinement effect as oxygen reduction electrocatalysts, *Nano Res.*, 2019, **12**, 2614-2622.

12 J. Zhang, G. Zhang, S. Jin, Y. Zhou, Q. Ji, H. Lan, H. Liu and J. Qu, Graphitic N in nitrogen-doped carbon promotes hydrogen peroxide synthesis from electrocatalytic oxygen reduction, *Carbon*, 2020, **163**, 154-161.

13 H. Sheng, E. D. Hermes, X. Yang, D. Ying, A. N. Janes, W. Li, J. R. Schmidt and S. Jin, Electrocatalytic production of H_2O_2 by selective oxygen reduction using earth-abundant cobalt pyrite (CoS_2), *ACS Catal.*, 2019, **9**, 8433-8442.

14 X. Lu, D. Wang, K. H. Wu, X. Guo and W. Qi, Oxygen reduction to hydrogen peroxide on oxidized nanocarbon: identification and quantification of active sites, *J. Colloid Interface Sci.*,

2020, **573**, 376-383.

15   X. Xiao, T. Wang, J. Bai, F. Li, T. Ma and Y. Chen, Enhancing the selectivity of H_2O_2 electrogeneration by steric hindrance effect, *ACS Appl. Mater. Interfaces*, 2018, **10**, 42534-42541.

16   H. Sheng, A. N. Janes, R. D. Ross, D. Kaiman, J. Huang, B. Song, J. R. Schmidt and S. Jin, Stable and selective electrosynthesis of hydrogen peroxide and the electro-fenton process on $CoSe_2$ polymorph catalysts, *Energy Environ. Sci.*, 2020, **13**, 4189-4203.